JACS
JOURNAL OF THE AMERICAN CHEMICAL SOCIETY

pubs.acs.org/JACS

Article

Mechanism of Electrochemical Generation and Decomposition of Phthalimide-*N*-oxyl

Cheng Yang, Luke A. Farmer, Derek A. Pratt,* Stephen Maldonado,* and Corey R. J. Stephenson*

Cite This: *J. Am. Chem. Soc.* 2021, 143, 10324−10332

Read Online

ACCESS | Metrics & More | Article Recommendations | Supporting Information

ABSTRACT: Phthalimide *N*-oxyl (PINO) is a potent hydrogen atom transfer (HAT) catalyst that can be generated electrochemically from *N*-hydroxyphthalimide (NHPI). However, catalyst decomposition has limited its application. This paper details mechanistic studies of the generation and decomposition of PINO under electrochemical conditions. Voltammetric data, observations from bulk electrolysis, and computational studies suggest two primary aspects. First, base-promoted formation of PINO from NHPI occurs via multiple-site concerted proton−electron transfer (MS-CPET). Second, PINO decomposition occurs by at least two second-order paths, one of which is greatly enhanced by base. Optimal catalytic efficiency in PINO-catalyzed oxidations occurs in the presence of bases whose corresponding conjugate acids have pK_a's in the range of ∼11−15, which strikes a balance between promoting PINO formation and minimizing its decay.

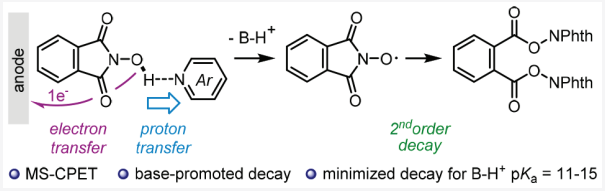

INTRODUCTION

Electrocatalysts that promote anodic half reactions have been specifically developed for oxidative organic transformations due to longstanding industrial interest.[1] The use of oxidative electrocatalysts, shuttling electrons between molecular substrates and anode interfaces, have realized chemical transformations in an environmentally friendly manner, as electrons are collected by electrode interfaces instead of stoichiometric chemical oxidants.[2] For example, the electrochemically generated *N*-oxoammonium ion derived from 2,2,6,6-tetramethylpiperidine-*N*-oxyl (TEMPO) serves as an active catalytic species and readily reacts with alcohols to produce carbonyls.[3] Both TEMPO and TEMPO$^+$ salts are isolable, which facilitates mechanistically guided development of this and related redox mediators for selective and efficient oxidations.[3]

PINO is another promising electrocatalyst generated by the facile oxidation of its precursor NHPI (Figure 1A).[3] PINO can abstract allylic[4] and benzylic[5−7] hydrogen atoms, as well as the other relatively weak C−H bonds,[8] making it a potential HAT electrocatalyst. However, PINO is short-lived, which has caused a limited operational utility for methodology development due to PINO decomposition.[8] The practical consequence of this decomposition is the need to use NHPI at high catalyst loading (10−20 mol %) to achieve efficient reactivity, as exemplified in the application to the oxidation of β-O-4 linkages in lignin.[6] Furthermore, the short lifetime of PINO has made mechanistic studies challenging.[3] Despite the interest in the NHPI/PINO couple as a valuable redox mediator,[3] a full assessment of off-cycle (i.e., PINO decomposition) pathways has not been performed.

PINO decomposition under electrochemical conditions was first reported by Masui and co-workers in 1987.[9] A trimeric

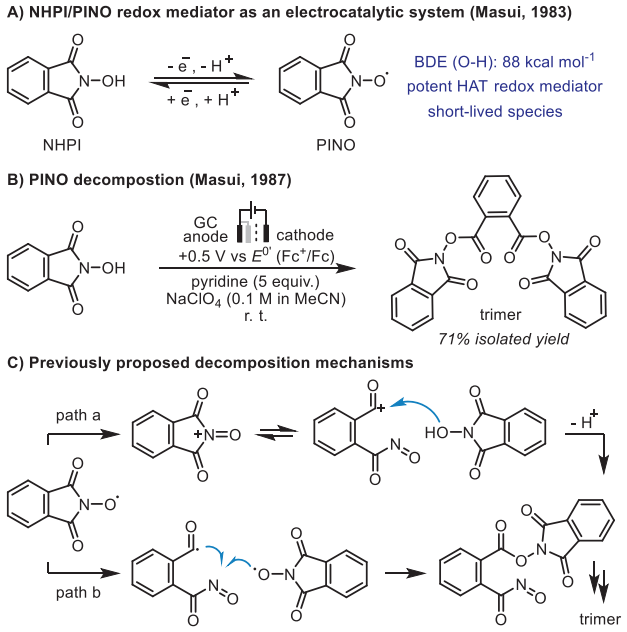

Figure 1. Previous studies on PINO decomposition under electrochemical conditions.

Received: April 21, 2021
Published: July 2, 2021

Downloaded via WASHINGTON UNIV on September 4, 2021 at 14:36:34 (UTC).
See https://pubs.acs.org/sharingguidelines for options on how to legitimately share published articles.

© 2021 American Chemical Society

https://doi.org/10.1021/jacs.1c04181
J. Am. Chem. Soc. 2021, 143, 10324−10332

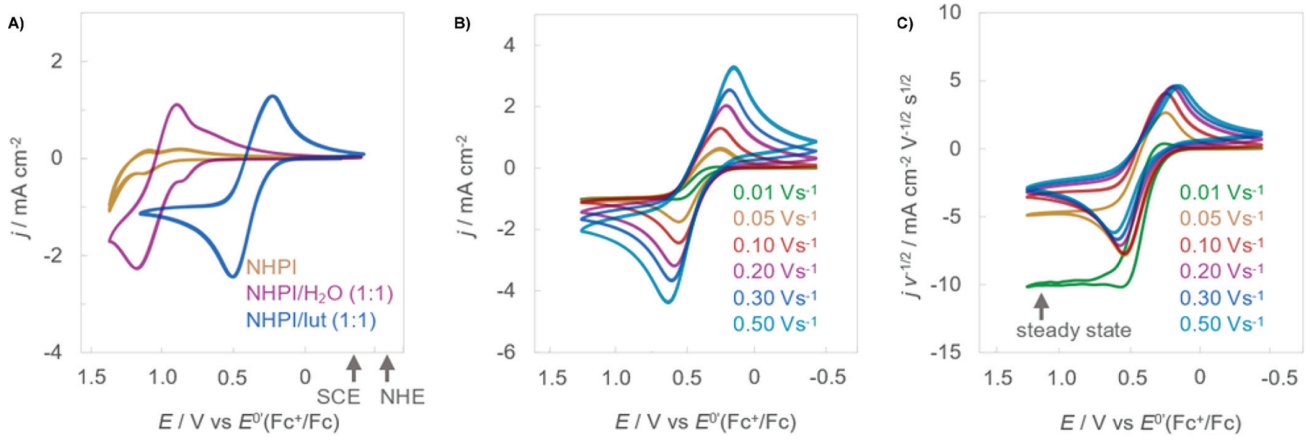

Figure 2. (A) Cyclic voltammograms for oxidation of 10 mM NHPI (yellow); in the presence of 10 mM water (purple); in the presence of 10 mM 2,6-lutidine (blue) at the scan rate of 0.1 V s^{-1}. (B,C) Cyclic voltammograms for oxidation of 10 mM NHPI in the presence of 10 mM 2,6-lutidine at the scan rate varying from 0.01 to 0.5 V s^{-1}.

species (hereafter trimer) was isolated and characterized as the major PINO decomposition product after bulk electrolysis of NHPI in the presence of pyridine (Figure 1B). The formation of the trimer by nucleophilic attack of NHPI upon its oxoammonium ion was suggested (Figure 1C, path a). Later, Pedulli and co-workers proposed a separate radical pathway involving coupling between PINO and the acyl radical arising from C−N bond fragmentation of another PINO (Figure 1C, path b).[10] Both decomposition pathways have been presumed as relevant in the literature without detailed scrutiny. Advancing NHPI/PINO as the redox mediator in an efficient catalytic system requires disambiguation of the PINO decomposition mechanisms.

To enable development of new strategies for selective electrochemical oxidation using NHPI or similar species, we have examined elementary aspects of PINO generation, and ascertained how it participates in oxidation of benzylic alcohols using electroanalytical and computational methods. The data indicate a multiple-site concerted proton−electron transfer (MS-CPET) mechanism of PINO generation from NHPI, where the proton and electron move to different locations.[11] Moreover, it suggests that in lieu of the two aforementioned mechanistic proposals for the decomposition of PINO, electrochemically generated PINO undergoes two distinct second-order decay processes, one of which is promoted by base. The influence of base strength on the catalytic efficiency of benzylic alcohol oxidation is quantitively analyzed. Taken together, this study provides a foundation for the development of more effective *N*-oxyl electrocatalysts.

RESULTS

Redox Response of NHPI with/without Bases. The redox response of NHPI at a glassy carbon electrode was measured in anhydrous MeCN with recrystallized tetrabutylammonium hexafluorophosphate (NBu_4PF_6).[12] Figure 2A shows the voltammetric response of NHPI without base in the electrolyte. In contrast to numerous previous reports, including our own,[4−7,13,14] a reversible voltammetric response was not observed. Instead, NHPI could not be readily oxidized at 0.1 V s^{-1} in this potential range under anhydrous conditions. Moreover, the lack of cathodic current on the return sweep suggested oxidized NHPI ($NHPI^{\bullet+}$) was unstable on this time scale. The redox response of NHPI oxidation speaks against a common assumption that NHPI can be reversibly oxidized both with and without a Brønsted base.[4−7,13,14]

Variation in the electrolyte did not affect the voltammetric response of NHPI unless care was not taken to exclude water (Supporting Information, SI). Adventitious and/or intentional addition of water to the electrolyte caused the voltammetric response to appear quasi-reversible, implicating water as an active agent during the oxidation of NHPI and suggesting similar wet conditions were likely used in prior reports of electrochemical oxidation of NHPI without added base.[4−7,13,14] In fact, we discovered that leakage of water (H_2O) from an aqueous reference electrode was sufficient to cause quasi-reversible behavior. The formal standard potential for NHPI oxidation in the presence of added H_2O, as determined from the midpoint of the redox waves ($E^{0'} \approx E_{1/2}$), was a function of the concentration of added water (SI). When one equivalent of water was used, $E_{1/2}$ = +1.04 V versus $E^{0'}(Fc^+/Fc)$ (Figure 2A).[15]

Cyclic voltammetric responses for the oxidation of NHPI in the presence of 1 equiv of 2,6-lutidine were collected from 0.01 to 0.5 V s^{-1} (Figure 2B). Normalizing the current densities in Figure 2C by $\sqrt{v}$ highlighted the fact that the voltammetric response shape was sensitive to the experimental time scale, indicating the oxidation of NHPI was coupled with at least one additional chemical reaction. At scan rates ≤0.01 V s^{-1}, the voltammetric response became sigmoidal, attaining a steady-state current density (Figure 2C) that suggested redox active species were being generated at the electrode by follow-up reactions in solution. A steady-state current density with the same magnitude was observed consistently for bases with pK_a values <15 and was insensitive to base concentration; see Supporting Information for further details.

To examine the possible contribution of inner-sphere effects in the redox responses, voltammetric measurements were performed with anodically activated glassy carbon.[16] However, this deliberate change in electrode surface chemistry did not impact the primary voltammetric features, as the observed peak splitting was invariant with the nature of the glassy carbon surface; see Supporting Information for further details.

NHPI-Base Complex. Identification of any possible reactions between NHPI and base was performed first, as most PINO-catalyzed oxidations are carried out in the presence of bases. When one equivalent of 2,6-lutidine was

https://doi.org/10.1021/jacs.1c04181
J. Am. Chem. Soc. 2021, 143, 10324−10332

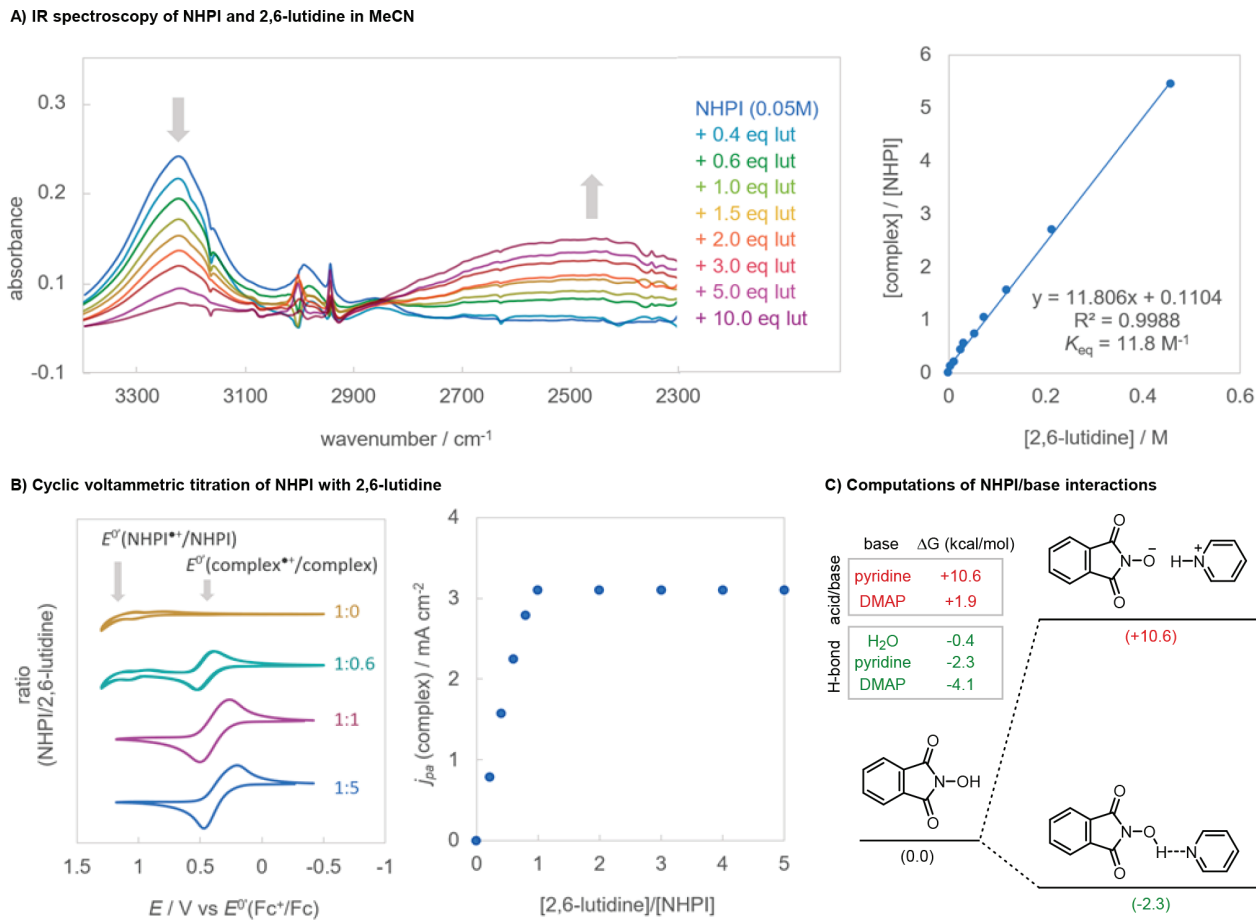

Figure 3. (A) IR spectroscopy of 0.05 M NHPI in MeCN, followed by addition of 2,6-lutidine. (B) Selected cyclic voltammograms for titration of 10 mM NHPI with 2,6-lutidine from 0 to 5 equiv at 0.1 V s^{-1} and the anodic current density as a function of ratio of [2,6-lutidine]/[NHPI]. (C) The free energy of the formation of the conjugate acid of NHPI, NHPI/base complex formation (B3LYP/6-311+G(d) with IEFPCM (MeCN)).

used as base, a quasi-reversible voltammogram was obtained with $E_{1/2}$ = +0.39 V versus $E^{0'}(Fc^+/Fc)$ (Figure 2A). The presence of base decreased the standard potential and increased the reversibility of NHPI oxidation. The reported pK_a values of NHPI (23.5)[11] and the 2,6-lutidinium ion (14.1)[17] in MeCN suggest that proton exchange is highly unfavorable. Nevertheless, the plausibility of a hydrogen bond formation between NHPI and pyridine derivative was assessed through IR spectroscopy. NHPI in MeCN shows a characteristic broad O−H stretch at 3210 cm^{-1} (Figure 3A). Addition of 2,6-lutidine caused a decrease in this absorption and the appearance of a very broad absorption at ∼2450 cm^{-1}, corresponding to the O−H stretch of the hydrogen-bonded complex.[18] The cumulative spectra were consistent with an equilibrium constant K_{eq} = 11.8 M^{-1} for a hydrogen-bonded complex (Figure 3A).

To determine the stoichiometry of the hydrogen-bonded complex, cyclic voltammetric titration experiments were conducted at 0.1 V s^{-1} (Figure 3B). A solution of NHPI in MeCN was titrated with 2,6-lutidine. The quasi-reversible voltammetric response at ∼+0.4 V versus $E^{0'}(Fc^+/Fc)$ corresponding to oxidation of the NHPI−lutidine complex grew in magnitude as the concentration of 2,6-lutidine increased with a concomitant disappearance of the voltammetric response observed in the absence of a base. The anodic peak current density for the oxidation of the complex was saturated until one equivalent of 2,6-lutidine was added, suggesting NHPI and 2,6-lutidine form a 1:1 complex in solution (Figure 3B). The $E_{1/2}$ was dependent upon the concentration of 2,6-lutidine (SI), consistent with pre-equilibrium complexation.

A set of calculations on the energies for both an ion pair of deprotonated NHPI and pyridinium and for a hydrogen-bonded complex was performed (Figure 3C). The free energy change corresponding to the formation of the 1:1 hydrogen-bonded complex between NHPI and pyridine was calculated to be −2.3 kcal/mol, rendering a formation constant (K_f) of 47.9. In reasonable agreement with this computation, Abraham's hydrogen-bonding parameters determined for pyridine (β_2^H = 0.62)[19] and NHPI (α_2^H = 0.37)[20] yield an estimate a K_f of 3.9.[21] In contrast, the Brønsted acid−base reaction (i.e., deprotonation) was predicted to be highly endergonic (ΔG = +10.6 kcal/mol). With 4-dimethylamino-pyridine (DMAP), deprotonation was expectedly more favorable compared to pyridine but still calculated to be endergonic (ΔG = +1.9 kcal/mol). Similarly, the formation of a NHPI−DMAP H-bonded complex is more thermodynamically favored (ΔG = −4.1 kcal/mol) than its NHPI−pyridine counterpart. The smaller ΔG between full deprotonation and NHPI−DMAP formation (+6.0 kcal/mol) is consistent with the higher pK_a of DMAP's conjugate acid (17.7).[17]

https://doi.org/10.1021/jacs.1c04181
J. Am. Chem. Soc. 2021, 143, 10324−10332

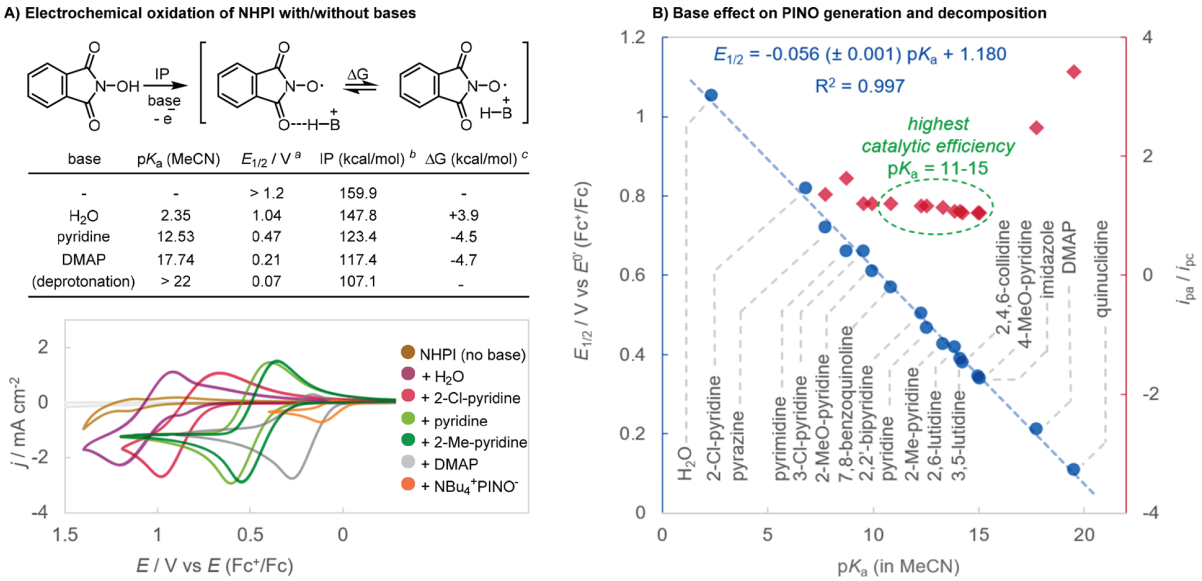

Figure 4. (A) (*a*) Selected cyclic voltammograms and calculations for oxidation of NHPI with/without base. (*b*,*c*) $E_{1/2}$ for oxidation of NHPI in the presence of 1 equiv of base 0.1 V s^{-1}. IP for oxidation of NHPI complexes, and free energy of dissociation of PINO and the associated conjugate acid (B3LYP/6-311+G(d) with IEFPCM (MeCN)). (B) $E_{1/2}$ versus pK_a (blue) and i_{pa}/i_{pc} versus pK_a (red).

Base Effect. To further probe the role of base in PINO generation and decomposition, a series of experiments were carried out with organic bases whose conjugate acids have well-defined pK_a values in MeCN.[17] Cyclic voltammograms for the oxidation of NHPI in the presence of one equivalent of different organic bases were collected at 0.1 V s^{-1} (selected examples presented in Figure 4A, the others in SI). In the presence of stronger bases, NHPI was oxidized at less positive potentials. The dependence of the $E_{1/2}$ values on pK_a are summarized in Figure 4B (blue filled circles). Across a pK_a range of 2 to 19, the linear least-squares fit yielded a slope of 56 ± 1 mV per pK_a unit, consistent with the Nernst factor ($2.303 \times RT/nF$ = 59 mV/pK_a) for proton-coupled electron transfer (PCET).[11]

A separate analysis of the apparent electron transfer rate constant (k^0) for each voltammogram in Figure S7 did not yield an obvious trend with pK_a. A likely factor was the differences in steric crowding around the pyridine nitrogen atom. For example, voltammetry with bipyridine yielded a much smaller k^0 value in comparison to pyridine, despite both voltammograms showing similar $E_{1/2}$.

Besides the potential shift, we also observed that the magnitude of the cathodic peak current varied with base strength (Figure 4A). Across these organic bases, the ratio of the anodic and cathodic peak current (i_{pa}/i_{pc}) was a function of the pK_a of the base, approaching 1 as the pK_a increased to 15 and then increasing at larger pK_a values (Figure 4B, red filled circles). In the presence of stronger bases, for example, DMAP and quinuclidine, the oxidation was irreversible. While the role of base as a proton acceptor is generally recognized,[4−8,11] the reason for the erosion of the reversibility of the electrochemical oxidation is not immediately apparent. On the basis of the lack of reversibility above a certain range of pK_a, it would seem that at least under electrochemical conditions, the decomposition of PINO is accelerated under increasingly basic conditions.

In an effort to delineate the effects of individual bases, the redox response of the conjugate base of NHPI (i.e., $PINO^-$) was determined. An NHPI salt, tetrabutylammonium phthalimide-*N*-oxide, was prepared[22] and its cyclic voltammogram was collected at 0.1 V s^{-1} in MeCN. Taking $E_{1/2}$ to be diagnostic of the formal potential, these data implied $E^{0\prime}$ ($PINO/PINO^-$) = +0.07 V versus $E^{0\prime}(Fc^+/Fc)$ (Figure 4A). The small cathodic peak further suggested PINO itself is unstable on the time scale of the voltammetry.[23] On the basis of the cumulative $E_{1/2}$ versus pK_a data, the voltammetry indicates a pK_a of ∼19 for NHPI in MeCN.

For additional insight on the effect of base on electrochemical oxidation, we expanded the computations in Figure 3C to compare oxidation of NHPI, the H-bonded complexes thereof, and $PINO^-$ (Figure 4A). Expectedly, NHPI was the most difficult species to oxidize, followed by the hydrogen-bonded complexes, and finally $PINO^-$. Importantly, the H-bonded complexes of NHPI and either pyridine or DMAP were predicted to decrease the ionization potential by 24.4 and 30.4 kcal/mol, respectively, relative to the NHPI−water complex. The decrease in ionization potential (IP) parallels the trend of decreasing standard potential for oxidation of NHPI observed experimentally, though a lack of quantitative agreement is not surprising given the absence of implicit solvation, which is presumably particularly relevant in the case of water. Notably, the complexes resulting from oxidation (i.e., PINO−H−base$^+$) were found to favor dissociation (ΔG = −4.5 and −4.7 kcal/mol, respectively), rendering pyridinium or dimethylaminopyridinium and free PINO. Hence, the increased reversibility of NHPI oxidation in the presence of pyridine does not appear to be due to product complexes which increase the persistence of PINO.

A test substrate, 1-phenylethanol, was used to assess whether the base affects the catalytic efficiency. A catalytic current enhancement was observed when the substrate was added to a solution of NHPI and organic bases (pK_a < 15) (SI). The catalytic current was independent of the pK_a of the base (SI). Importantly, no current enhancement was observed when stronger bases (i.e., DMAP, NEt_3 or quinuclidine) were used. Comparing the catalytic currents measured for 1-phenylethanol and 1-phenylethanol-d_1 yielded a kinetic isotope effect

https://doi.org/10.1021/jacs.1c04181
J. Am. Chem. Soc. 2021, 143, 10324−10332

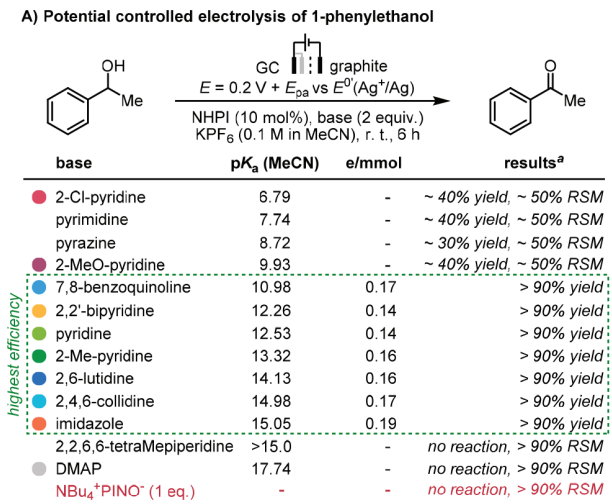

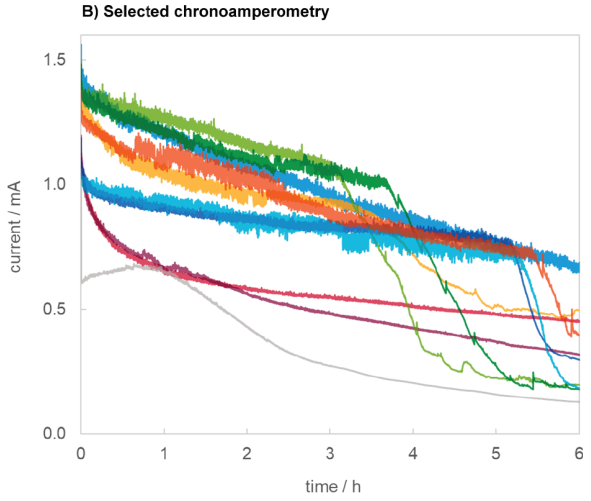

Figure 5. (A) Electrolysis conditions: 1-phenylethanol (0.16 mmol), NHPI (10 mol %, 0.016 mmol), base (2 equiv., 0.32 mmol), KPF_6 (0.1 M in 8 mL MeCN), open-air, divided cell, glassy carbon plate anode (2 cm^2), graphite cathode (4 cm^2), potential controlled electrolysis (0.2 V more positive than anodic peak potential for each redox couple). (*a*) RSM = remaining starting material. Yields determined by GC-MS. (B) Chronoamperometry recorded by potentiostat.

of 1.8, suggesting that the abstraction of the benzylic hydrogen atom is rate-determining in the electrochemical oxidation (SI).

Electrolyses of 1-phenylethanol catalyzed by NHPI were performed in the presence of different bases at a constant potential for 6 h (Figure 5). The potential was set to +0.2 V relative to the anodic peak potential for each redox couple. The resulting solutions were analyzed by gas chromatography coupled to a mass spectrometer (GC-MS). The best catalytic efficiency was observed for bases with a pK_a within the range of ~11 to 15 with full conversion within 6 h. Studying the reaction by integrating chronocoulometry (i.e., charge as a function of time) indicated that ~1 equiv of electrons passed through the cell, suggesting the absence of chain reactions.[24] The correlation of reaction time and base strength was in line with the following premise: Weaker bases (pK_a < 10) displayed a current drop during the reaction and low conversions were obtained. On the other hand, stronger bases (pK_a > 17) were ineffective for catalysis, resulting in no desired oxidation. Consistent with the foregoing, electrolysis of 1-phenylethanol in the presence of 1 equiv of the NHPI salt resulted in >90% recovery of the starting material. A substituent effect was noted, as the current magnitude and time to reach full conversion was dependent upon the steric bulk of the base. The less sterically hindered bases gave higher currents and shorter reaction times. However, when the pK_a was above 15, even sterically hindered bases (e.g., 2,2,6,6-tetramethylpiperidine) were not able to promote the oxidation.

Mechanistic Insights on PINO Decomposition. To understand the causes of catalyst decomposition in order to develop more efficient catalytic systems, PINO decomposition was investigated using computational methods to interrogate both the existing mechanistic proposals as well as others which we considered plausible. Initially, we examined the second-order decay originally proposed by Masui (Figure 1C, path a).[9] This decomposition path proceeds first by disproportionation of two molecules of PINO as the (presumed) rate-determining step. The resulting oxoammonium $PINO^+$ (**2**) could then undergo acyl substitution by either NHPI or its conjugate base $PINO^-$ to yield the putative dimeric intermediate, which could subsequently lead to the isolated trimer (vide infra). Unlike the oxoammonium ion derived from TEMPO, $PINO^+$ has not yet been reported in the literature. Indeed, the computed free energy difference between two molecules of PINO and $PINO^-$ + $PINO^+$ (ΔG = +51.9 kcal/mol, Figure 6, path a) suggests

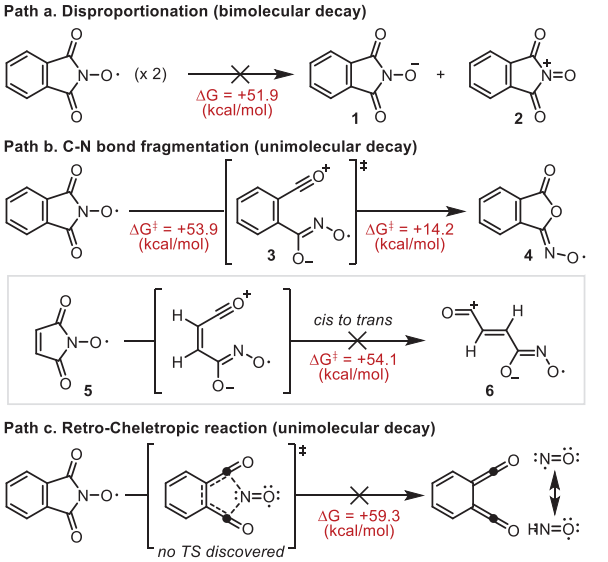

Figure 6. Reaction pathways initially considered for decay of PINO (B3LYP/6-311+G(d) with IEFPCM (MeCN)).

that disproportionation is highly endergonic. Furthermore, the IP of PINO was computed to be highly similar to that of NHPI (ΔG = +158.6 vs +159.9 kcal/mol), suggesting that the potential required for anodic oxidation would be well beyond the potential at which oxidation of the NHPI-base complex occurs. On this basis, the formation of a discrete intermediate **2**, as originally depicted by Masui, is unlikely to occur.

The previously suggested C−N fragmentation was also examined (Figure 1C, path b).[10] The only productive mode of C−N cleavage identified by computational means was through the rotation of one of the C(aryl)−C(acyl) bonds (Figure 6, path a), which led to a high energy charge-separated activated

https://doi.org/10.1021/jacs.1c04181
J. Am. Chem. Soc. 2021, 143, 10324−10332

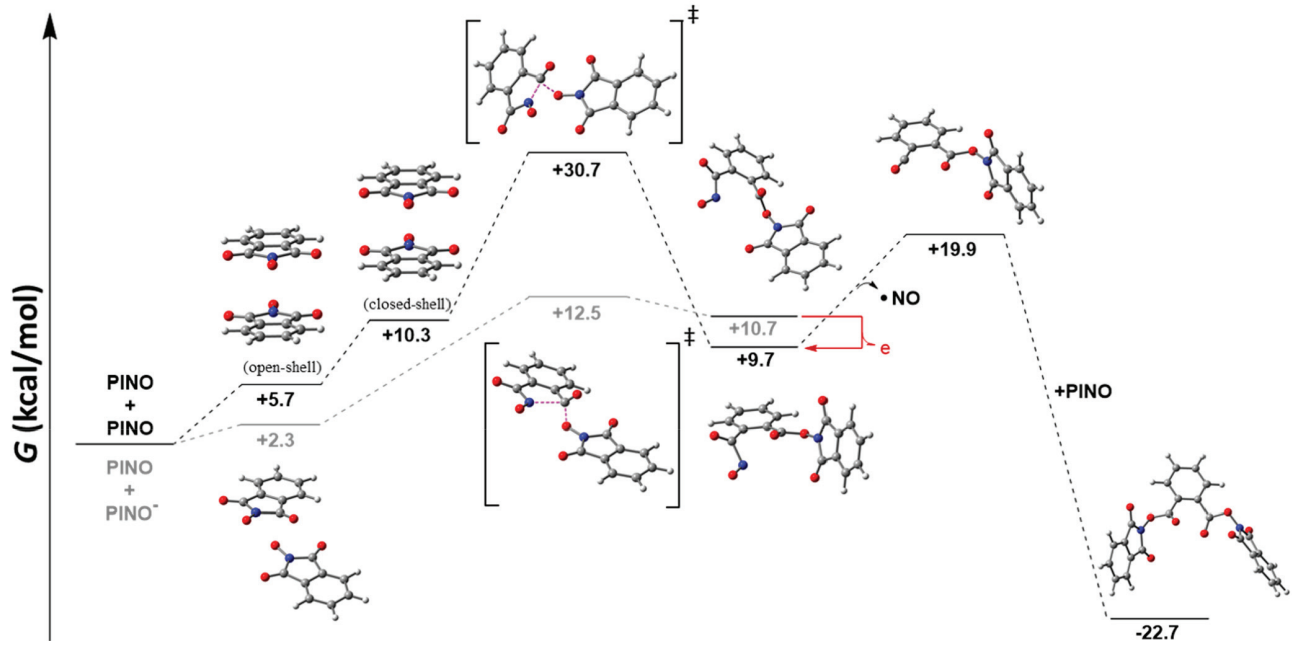

Figure 7. Free energy diagram of proposed bimolecular decomposition pathways of PINO (B3LYP/6-311+G(d) with IEFPCM (MeCN) and GD3 empirical dispersion correction).

complex **3** with acylium cation and amide anion *N*-oxyl moieties (ΔG = +53.9 kcal/mol), not an acyl radical. Intrinsic reaction coordinate (IRC) calculations revealed that this transition state collapses to phthalic anhydride monoimine-*N*-oxyl **4**, obviously a consequence of the conformational restriction imposed on the reactive moieties by the aryl ring to which they are attached. To provide some insight on the intrinsic strength of the C−N bond in question, we determined the energy difference between maleimide-*N*-oxyl **5** and the (*E*)-isomer of its C−N bond fragmentation product **6** (Figure 6, path b). This transformation has essentially the same free energy cost as formation of the activated complex of PINO heterolysis (ΔG = +54.1 kcal/mol). The results imply that the suggested C−N bond cleavage is also unlikely to occur under relevant conditions. In addition, the concerted fragmentation of both C−N bonds analogous to the reverse reaction of quinone dimethide-based nitric oxide cheletropic traps (NOCTs) was considered (Figure 6, path c).[25] Although a transition state was not found, considering the endergonicity of this reaction (ΔG = +59.3 kcal/mol), it is also unlikely to contribute to the decay of PINO. Admittedly, this point is perhaps not surprising given NOCT reactions have not been reported as being reversible.

Considering the modes by which two molecules of PINO may dimerize, a lower energy pathway similar to Masui's original disproportionation proposal was found (Figure 7). An activated complex corresponding to the combination of $PINO^-$ and $PINO^+$ was identified with ΔG = +36.5 kcal/mol relative to two isolated PINO molecules and is much lower in energy than the sum computed from the energies of the discrete $PINO^-$ and $PINO^+$ ions (ΔG = +51.9 kcal/mol, Figure 6A). IRC calculations suggest that this transition state connects Masui's aforementioned dimeric intermediate to a PINO contact ion pair at ΔG = +16.8 kcal/mol relative to two isolated PINO molecules. It seems reasonable to suggest that this contact ion pair results from charge transfer from a corresponding PINO radical pair to avoid formation of the higher energy separated $PINO^-$ and $PINO^+$ ions. Indeed, the corresponding PINO (singlet) radical pair is 7.0 kcal/mol lower in free energy than the contact ion pair. Suspecting that the free energy difference between the PINO radical pair and two separated PINO radicals (9.8 kcal/mol) was overestimated on account of DFT's failure to account for dispersion interactions, we incorporated Grimme's empirical dispersion correction (GD3)[26] in our calculations. Doing so led to a decrease in the free energy change for association of the PINO radical pair (to +5.7 kcal/mol), the contact ion pair (to +10.3 kcal/mol) and overall barrier for substitution (to +30.7 kcal/mol); see Supporting Information for further details.

Given the lack of reversibility observed when the tetrabutylammonium salt of NHPI is oxidized or when stronger bases are present, we wondered if $PINO^-$ may attack PINO directly. Indeed, a comparatively low energy transition state structure was readily identified for this substitution (Figure 7). The transition state was characterized by significant O−C bond formation and C−N bond cleavage. IRC calculations revealed that this structure connected a PINO/$PINO^-$ complex and the substitution product independent of a tetrahedral intermediate. Again, inclusion of the GD3 empirical dispersion correction systematically decreased the overall computed free-energy barrier from +17.9 to +12.5 kcal/mol. Although, as in the case of the reaction of two PINO molecules, the reaction is endergonic (ΔG = +10.7 kcal/mol), the resultant amide anion *N*-oxyl should oxidize readily since its ionization potential is essentially equivalent to that calculated for $PINO^-$ (ΔG = 106.3 vs 107.1 kcal/mol, respectively).[27] This oxidation would generate Masui's proposed dimeric intermediate.

The optimized structure of Masui's proposed dimer was characterized by a conspicuously long C−N bond between the carbonyl carbon and nitroso nitrogen atoms (1.59 Å), implying it to be quite weak. Indeed, the calculated bond dissociation

https://doi.org/10.1021/jacs.1c04181
J. Am. Chem. Soc. 2021, 143, 10324−10332

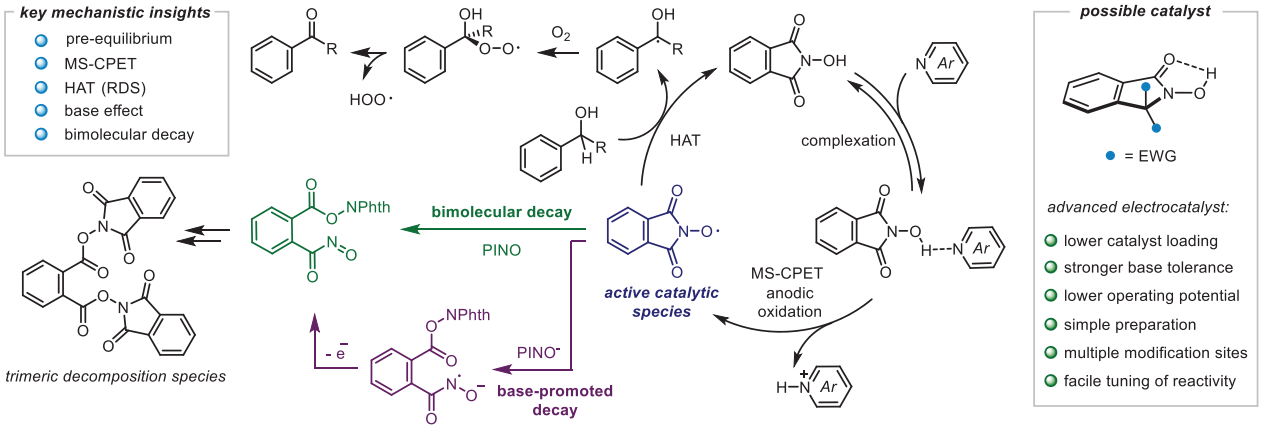

Figure 8. Mechanisms of the electrochemical generation and decomposition of PINO.

free energy (BDFE) is +10.2 kcal/mol, implying the homolysis would occur readily under the reaction conditions, releasing nitric oxide. The incipient acyl radical could be trapped by PINO in a reaction that is predicted to be 42.6 kcal/mol downhill.[28] It should be noted that, in absolute terms, the B3LYP/6-311+G(d) method used for the foregoing calculations is likely to underestimate these bond strengths. Therefore, to provide further insight, we carried out high accuracy CBS-QB3 calculations on a model wherein the "spectator" PINO moiety is replaced with a hydroxyl group, which yielded corresponding free energies of +15.1 and −58.7 kcal/mol, respectively).[29] Nevertheless, the results support a transitory "dimeric" intermediate and a stable "trimeric" product in line with the observations made to date.

Considering the PINO decomposition mechanism is base promoted, the decomposition rate must be base dependent. A series of low scan rate cyclic voltammetric measurements was performed at 0.01 V s^{-1} as in Figure 2c. Among these investigated bases, the steady-state currents were observed consistently (SI). With weak bases (pK_a < 15), the steady-state current was independent of base strength and base concentration. When stronger bases (pK_a > 15) were used, the steady-state current was proportional to the base concentration. Taking this information together, we posit that the observed steady state current indicated that PINO decomposition produces a new redox active species that is easier to oxidize. These voltametric observations are therefore in agreement with aforementioned computational studies.

DISCUSSION

The presented data speak to the following three points. First, PINO-catalyzed electrochemical oxidation occurs by a MS-CPET mechanism. Second, the reversibility of electrochemical oxidation of NHPI is dependent on the added base strength, and consequently the base strength affects the conversion efficiency of the electrocatalytic oxidation of 1-phenylethanol. Third, PINO decomposition is promoted by base via nucleophilic substitution by $PINO^-$ on a carbonyl of a second PINO followed by single electron oxidation of the resultant complex.

The linear dependence of $E_{1/2}$ on pK_a with a slope of 56 ± 1 mV/pK_a, observed for the oxidation of NHPI in the presence of base, is a hallmark of PCET reactions.[11] Indeed, Mayer and co-workers have suggested MS-CPET as a plausible mechanism for the base-mediated formation of PINO from NHPI, in analogy to their study on base mediated oxidation of *N*-hydroxy-2,2,6,6-tetramethylpiperidine (TEMPO-H).[18] The $E_{1/2}$ versus pK_a correlation addresses two further aspects. First, these data indicate that $E^{0'}(NHPI^{\bullet+}/NHPI)$ is ≥+1.05 V versus $E^{0'}(Fc^+/Fc)$, in agreement with prior predictions from theory.[11] Second, these data indicate that $E^{0'}(PINO/PINO^-)$ is closer to +0.07 V versus $E^{0'}(Fc^+/Fc)$ − which is slightly more positive than prior theoretical predictions of $E^{0'}(PINO/PINO^-)$ = −0.1 V versus $E^{0'}(Fc^+/Fc)$.[11] Similarly, the cumulative voltammetric measurements shown here indicate that the pK_a of NHPI in MeCN is 19 (rather than 23.5).[11]

The subject of PINO decomposition has been a matter of interest since the seminal kinetic studies conducted by Masui,[9] although the details have remained hitherto nebulous. Both first[30] and second order decay[9,31] with respect to PINO have been reported leading to a bifurcation of proposed decay processes that have been presumed to lead to the same trimer decomposition product.[8] Our data suggests that ascribing the observed first-order decay[30] of PINO to a unimolecular phenomenon perhaps takes too much for granted. The underlying assumption is that the principal product of the process is the same trimer previously observed by Masui. Additionally, as pointed out by Pedulli, the kinetics of decay are quite dependent on solvent composition,[30a] an observation which seems inconsistent with unimolecular decay being rate-determining. However, without more information on the actual product(s) formed as a result of the first-order decay process(es), or the prerequisites for its occurrence, searching for the rate defining reaction *in silico* may be futile. Suffice to say, the oft-invoked fragmentation of the C−N bond in PINO to form a transient acyl radical which can be captured appears unlikely.

The presented data suggest that the strength of the base alters the catalytic efficiency by influencing PINO decomposition. The voltammetric measurements and electrolysis experiments suggest an optimal base strength in the pK_a range of ∼11−15. Specifically, we posit that PINO has two operative decomposition pathways in MeCN (Figures 7 and 8). One decomposition involves the dimerization of two molecules of PINO via a charge-transfer complex. In the presence of weak bases (pK_a < 15), this pathway is dominant. In the presence of comparatively strong bases (pK_a > 15), a second significantly faster decomposition pathway consisting of the reaction between $PINO^-$ and PINO is operative. The resulting intermediate is rapidly oxidized at the anode to produce the

https://doi.org/10.1021/jacs.1c04181
J. Am. Chem. Soc. 2021, 143, 10324−10332

same dimer. This oxidation event is observable at slow scan rates. The dimer undergoes C−N cleavage to release nitric oxide and form an acyl radical which reacts with another molecule of PINO to form the observed trimer.

Our expansion on early observations regarding base-promoted oxidations and elucidation of a reasonable PINO decomposition mechanism provides guidance to advance PINO-catalyzed electrochemical oxidations. Previous efforts to design improved PINO-like HAT catalysts have largely focused on adjusting BDFEs—up to yield a more reactive catalyst or down to yield a more selective catalyst. In contrast, an approach to improving catalysis through extension of the effective catalytic lifetime of PINO by obviating degradation pathways has not been a focus of research efforts. On the basis of the results presented herein, we suggest that both of these aspects should be considered in the design of more effective *N*-oxyl catalysts for C−H oxidation reactions.

Furthermore, we posit the following directions for future *N*-oxyl catalyst development. First, it is of great importance to develop electrocatalysts compatible with strong bases. Avoiding rapid base-promoted decay will allow one to operate reactions at lower applied potentials using stronger bases, which will result in a broader substrate scope and an extension to the reactions that require stronger bases for which NHPI is poorly suited. Considering the electrophilic carbonyl is key to decomposition, replacing one or both carbonyls with other electron-withdrawing functional groups could solve this problem. Second, strategic design of electrocatalysts with a much slower bimolecular decay should be pursued. The resulting longer lifetime of the catalyst will improve such oxidation reactions by decreasing catalyst loading. Rendering the carbonyls less electrophilic could be a way to decrease bimolecular decay. Studies in these directions are ongoing in our laboratories.

CONCLUSION

In summary, we have described a comprehensive electroanalytical study of the NHPI/PINO redox mediator and conducted computational studies to uncover the mechanisms by which PINO degrades as a function of the identity of the base. The data provides a roadmap for developing more effective *N*-oxyl catalysts for C−H oxidation reactions.

ASSOCIATED CONTENT

Supporting Information

The Supporting Information is available free of charge at https://pubs.acs.org/doi/10.1021/jacs.1c04181.

Cyclic voltammetry, electrolysis, compound characterization, and calculations (PDF)

AUTHOR INFORMATION

Corresponding Authors

Derek A. Pratt − *Department of Chemistry and Biomolecular Sciences, University of Ottawa, Ottawa, Ontairo K1N 6N5, Canada;* orcid.org/0000-0002-7305-745X; Email: dpratt@uottawa.ca

Stephen Maldonado − *Willard Henry Dow Laboratory, Department of Chemistry, University of Michigan, Ann Arbor, Michigan 48109, United States; Program in Applied Physics, University of Michigan, Ann Arbor, Michigan 48109, United States;* orcid.org/0000-0002-2917-4851; Email: smald@umich.edu

Corey R. J. Stephenson − *Willard Henry Dow Laboratory, Department of Chemistry, University of Michigan, Ann Arbor, Michigan 48109, United States;* orcid.org/0000-0002-2443-5514; Email: crjsteph@umich.edu

Authors

Cheng Yang − *Willard Henry Dow Laboratory, Department of Chemistry, University of Michigan, Ann Arbor, Michigan 48109, United States*

Luke A. Farmer − *Department of Chemistry and Biomolecular Sciences, University of Ottawa, Ottawa, Ontairo K1N 6N5, Canada*

Complete contact information is available at: https://pubs.acs.org/10.1021/jacs.1c04181

Notes

The authors declare no competing financial interest.

ACKNOWLEDGMENTS

C.R.J.S. acknowledges the financial support from the National Science Foundation (CHE-1565782 and CBET-2033714), and the University of Michigan. S.M. acknowledges the generous support from the Department of Energy (DE-SC0006628). D.A.P. acknowledges the financial support from the Natural Sciences and Engineering Research Council of Canada. This work was enabled by support provided by Compute Ontario and Compute Canada (www.computecanada.ca).

REFERENCES

(1) Yan, M.; Kawamata, Y.; Baran, P. S. Synthetic Organic Electrochemical Methods Since 2000: On the Verge of a Renaissance. *Chem. Rev.* **2017**, *117*, 13230−13319.

(2) Moeller, K. D. Synthetic Applications of Anodic Electrochemistry. *Tetrahedron* **2000**, *56*, 9527−9554.

(3) Nutting, J. E.; Rafiee, M.; Stahl, S. S. Tetramethylpiperidine *N*-Oxyl (TEMPO), Phthalimide *N*-Oxyl (PINO), and Related *N*-Oxyl Species: Electrochemical Properties and Their Use in Electrocatalytic Reactions. *Chem. Rev.* **2018**, *118*, 4834−4885.

(4) Horn, E. J.; Rosen, B. R.; Chen, Y.; Tang, J.; Chen, K.; Eastgate, M. D.; Baran, P. S. Scalable and Sustainable Electrochemical Allylic C-H Oxidation. *Nature* **2016**, *533*, 77−81.

(5) Masui, M.; Ueshima, T.; Ozaki, S. *N*-Hydroxyphthalimide as an Effective Mediator for the Oxidation of Alcohols by Electrolysis. *J. Chem. Soc., Chem. Commun.* **1983**, 479−480.

(6) Bosque, I.; Magallanes, G.; Rigoulet, M.; Kärkäs, M. D.; Stephenson, C. R. J. Redox Catalysis Facilitates Lignin Depolymerization. *ACS Cent. Sci.* **2017**, *3*, 621−628.

(7) Rafiee, M.; Wang, F.; Hruszkewycz, D. P.; Stahl, S. S. *N*-Hydroxyphthalimide-Mediated Electrochemical Iodination of Methylarenes and Comparison to Electron-Transfer-Initiated C-H Functionalization. *J. Am. Chem. Soc.* **2018**, *140*, 22−25.

(8) Recupero, F.; Punta, F. Free Radical Functionalization of Organic Compounds Catalyzed by *N*-Hydroxyphthalimide. *Chem. Rev.* **2007**, *107*, 3800−3842.

(9) Ueda, C.; Noyama, M.; Ohmori, H.; Masui, M. Reactivity of Phthalimide-*N*-oxyl: A Kinetic Study. *Chem. Pharm. Bull.* **1987**, *35*, 1372−1377 Note: In Masui's report, the potential controlled electrolysis was performed at 0.9 V vs SCE, which is 0.52 V vs $E^{0'}$ (Fc^+/Fc) (see ref 15.)..

(10) Amorati, R.; Lucarini, M.; Mugnaini, V.; Pedulli, G. F.; Minisci, F.; Recupero, F.; Fontana, F.; Astolfi, P.; Greci, L. Hydroxylamines as Oxidation Catalysts: Thermochemical and Kinetic Studies. *J. Org. Chem.* **2003**, *68*, 1747−1754.

(11) Warren, J. J.; Tronic, T. A.; Mayer, J. M. Thermochemistry of Proton-Coupled Electron Transfer Reagents and its Implications. *Chem. Rev.* **2010**, *110*, 6961−7001. Note: The reported pK_a of NHPI

in MeCNis an extrapolated value based on the pK_a measured in DMSO as opposed to a direct measurement in MeCN. See: Kütt, A.; Leito, I.; Kaljurand, I.; Sooväli, L.; Vlasov, V. M.; Yagupolskii, L. M.; Koppel, I. A. A Comprehensive Self-Consistent Spectrophotometric Acidity Scale of Neutral Brønsted Acids in Acetonitrile. *J. Org. Chem.* **2006**, *71*, 2829−2838.

(12) Sawyer, D. T.; Hage, J. P.; Sobkowiak, A. *J. Am. Chem. Soc.* **1995**, *117*, 106.

(13) Kishioka, S.; Yamada, A. Kinetic Study of the Catalytic Oxidation of Benzyl Alcohols by Phthalimide-*N*-Oxyl Radical Electrogenerated in Acetonitrile using Rotating Disk Electrode Voltammetry. *J. Electroanal. Chem.* **2005**, *578*, 71−77.

(14) Rafiee, M.; Karimi, B.; Alizadeh, S. Mechanistic Study of the Electrocatalytic Oxidation of Alcohols by TEMPO and NHPI. *ChemElectroChem* **2014**, *1*, 455−462.

(15) 0 V vs $E^{0'}$ (Fc^+/Fc) = + 0.38 V vs SCE = + 0.63 V vs NHE. See: Pavlishchuk, V. V.; Addison, A. W. Conversion Constants for Redox Potentials Measured Versus Different Reference Electrodes in Acetonitrile Solutions at 25°C. *Inorg. Chim. Acta* **2000**, *298*, 97−102.

(16) Sawant, T. V.; McKone, J. R. Flow Battery Electroanalysis. 2. Influence of Surface Pretreatment on $Fe^{(III/II)}$ Redox Chemistry at Carbon Electrodes. *J. Phys. Chem. C* **2019**, *123*, 144−152.

(17) (a) Lõkov, M.; Tshepelevitsh, S.; Heering, A.; Plieger, P. G.; Vianello, R.; Leito, I. On the Basicity of Conjugated Nitrogen Heterocycles in Different Media. *Eur. J. Org. Chem.* **2017**, *2017*, 4475−4489. (b) Kaljurand, I.; Rodima, T.; Leito, I.; Koppel, I. A.; Schwesinger, R. Self-Consistent Spectrophotometric Basicity Scale in Acetonitrile Covering the Range between Pyridine and DBU. *J. Org. Chem.* **2000**, *65*, 6202−6208. (c) Kolthoff, I. M.; Ikeda, S. Polarographic and Acid Properties of Thorium Perchlorate in Acetonitrile. *J. Phys. Chem.* **1961**, *65*, 1020−1026. (d) iBonD 2.0 databank: http://ibond.nankai.edu.cn. Accessed on June 1st, 2020.

(18) Morris, W. D.; Mayer, J. M. Separating Proton and Electron Transfer Effects in Three-Component Concerted Proton-Coupled Electron Transfer Reactions. *J. Am. Chem. Soc.* **2017**, *139*, 10312−10319.

(19) Abraham, M. H.; Grellier, P. L.; Prior, D. V.; Morris, J. J.; Taylor, P. J. *J. Chem. Soc., Perkin Trans. 2* **1990**, *2*, 521−529.

(20) The K_f of NHPI with MeCN ($\beta_2^H = 0.44$)[18] is reported (1.3 M^{-1})[27a] from which the α_2^H of NHPI (0.37) is calculated ($\log K_f = 7.354\alpha_2^H\beta_2^H - 1.094$).

(21) While at first glance the 12-fold difference (1.5 kcal/mol) between the two predicted formation constants for the H-bonded complex between NHPI and pyridine seems quite large, we consider it remarkably good agreement given the two approaches. One is derived from empirical solvent H-bond acidity/basicity parameters derived from IR measurements with a variety of donor/acceptor combinations in CCl_4, and the other is derived from gas phase thermochemistry to which a solvent reaction field corresponding to the bulk electrostatic properties of acetonitrile has been applied.

(22) Dekamin, M. G.; Mokhtari, J.; Naimi-Jamal, M. R. Organocatalytic cyanosilylation of carbonyl compounds by tetrabutylammonium phthalimide-*N*-oxyl. *Catal. Commun.* **2009**, *10*, 582−585.

(23) The current magnitude for oxidation of the NHPI salt was smaller than the other NHPI/base complex. This was possibly due to a self-complexation between the ionic species, which was presented in the SI.

(24) It would appear that it is not a chain reaction, or the chain reaction is extremely short. We suspect this may be since the rate constant for reaction of a hydroperoxyl radical (HOO•) and benzylic alcohol substrate is so much slower than HOO• and PINO, which is presumably diffusion controlled given that the reaction between HOO• and TEMPO occurs with $k \sim 10^9$ M^{-1} s^{-1}. See: (a) Harrison, K. A.; Haidasz, E. A.; Griesser, M.; Pratt, D. A. Inhibition of hydrocarbon autoxidation by nitroxide-catalyzed cross-dismutation of hydroperoxyl and alkylperoxyl radicals. *Chem. Sci.* **2018**, *9*, 6068−6079. (b) Baschieri, A.; Valgimigli, L.; Gabbanini, S.; DiLabio, G. A.; Romero-Montalvo, E.; Amorati, R. Extremely Fast Hydrogen Atom Transfer between Nitroxides and HOO· Radicals and Implication for Catalytic Coantioxidant Systems. *J. Am. Chem. Soc.* **2018**, *140*, 10354. In fact, at the potential of the experiment HOO• is probably oxidized. See: Koppenol, W. H.; Stanbury, D. M.; Bounds, P. L. Electrode Potentials of Partially Reduced Oxygen Species, from Dioxygen to Water. *Free Radical Biol. Med.* **2010**, *49*, 317−322.

(25) Korth, H.-G.; Sustmann, R.; Lommes, P.; Paul, T.; Ernst, A.; de Groot, H.; Hughes, L.; Ingold, K. U. *J. Am. Chem. Soc.* **1994**, *116*, 2767−2777.

(26) Grimme, S.; Antony, J.; Ehrlich, S.; Krieg, H. A Consistent and Accurate *ab initio* Parameterization of Density Functional Dispersion Correction (DFT-D) for the 94 Elements H-Pu. *J. Chem. Phys.* **2010**, *132*, 154104.

(27) Shown is the IP for amide anion *N*-oxyl without GD3 correction applied, and it was found to have no impact on the computed value regardless (106.3 vs 106.1 kcal/mol).

(28) The DFT BDFE values were calculated both with and without GD3 empirical correction for the C−N of the dimer complex (+10.2/+7.2 kcal/mol respectively) and the C−O of the trimer complex (+42.1/+38.4 kcal/mol respectively). The former is highlighted in the main text for direct comparison with the bimolecular pathways described vide supra.

(29) The C−O and C−N BDE/BDFE values were calculated using a high accuracy CBS-QB3 method (gas-phase) with the phthalimide on the other carbonyl truncated to a hydroxyl group. Replacing the phthalimide with hydroxyl was found to have a negligible impact on the BDE/BDFE when using the B3LYP/6-311+G(d) method sans GD3 ($\leq$ 1.5 kcal/mol). The calculated C-O BDE/BDFE of the model trimer was 71.3/58.7 kcal/mol. The calculated C-N BDE/BDFE of the model intermediate dimer was 26.7/15.1 kcal/mol. For comparison, 26.7 kcal/mol is ∼10 kcal/mol lower than the O-O BDE of a typical alkyl peroxide. See: Bach, R. D.; Ayala, P. Y.; Schlegel, H. B. *J. Am. Chem. Soc.* **1996**, *118*, 12758−12765.

(30) (a) Amorati, R.; Lucarini, M.; Mugnaini, V.; Pedulli, G. M.; Minisci, F.; Recupero, F.; Fontana, F.; Astolfi, P.; Greci, L. *J. Org. Chem.* **2003**, *68*, 1747−1754. (b) Kushch, O.; Hordieieva, I.; Novikova, K.; Litvinov, Y.; Kompanets, M.; Shendrik, A.; Opeida, I. *J. Org. Chem.* **2020**, *85*, 7112−7124.

(31) (a) Koshino, N.; Saha, B.; Espenson, J. H. *J. Org. Chem.* **2003**, *68*, 9364−9370. (b) Baciocchi, E.; Gerini, M. F.; Lanzalunga, O. *J. Org. Chem.* **2004**, *69*, 8963−8966.

https://doi.org/10.1021/jacs.1c04181
J. Am. Chem. Soc. 2021, 143, 10324−10332